

# APPLICATION OF UAV AERIAL PHOTOGRAPHY TO TEMPOROSPATIAL ASSESSMENT OF TIDAL FLAT GEOMORPHOLOGY

Yoichi WATABE<sup>1</sup> and Shinji SASSA<sup>2</sup>

<sup>1</sup>Member of ISSMGE, Soil Mechanics and Geoenvironment Laboratory, Port and Airport Research Institute  
(3-1-1, Nagase, Yokosuka 239-0826, Japan)

E-mail:watabe@ipc.pari.go.jp

<sup>2</sup>Member of ISSMGE, Soil Mechanics and Geoenvironment Laboratory, Port and Airport Research Institute  
(3-1-1, Nagase, Yokosuka 239-0826, Japan)

E-mail:sassa@ipc.pari.go.jp

This study is aimed at developing a new technology, which uses an unmanned aerial vehicle (UAV) and digital photography, for the temporospatial geomorphology of intertidal flats. The UAV used in this study can be used for autonomous flights. Because of the tranquility of the water surface of the intertidal flats, the waterline (i.e., water edge) in the UAV aerial photographs corresponds to a very precise contour of the intertidal flats. High-resolution photographs are useful for studying the interrelations between geomorphology and bioactivity in the intertidal flats. The method developed is applicable to not only the geomorphology of natural intertidal flats but also artificial intertidal flats.

**Key Words :** remote sensing, tidal flat, geomorphology, UAV, waterline

## 1. INTRODUCTION

Intertidal flats are the key elements in coastal environments; they consist of regions with rich bioactivity and also contribute toward water purification. Most of the previous studies on issues associated with intertidal flats have been conducted on the basis of the following approaches: biological approach, hydrological approach, and chemical approach. Although the important characteristic of intertidal flats is that the exposed soils are the primary habitats for benthic life, most of these studies have mainly focused on the period of submergence.

Sassa and Watabe (2007) carried out continuous measurements in an intertidal sandy flat, and they closely captured the dynamics of suction ( $s = u_a - u_w$ , where  $u_a$  denotes the atmospheric air pressure and  $u_w$  denotes the pore water pressure) in shallow soils under tide-induced groundwater table fluctuations. They demonstrated that such suction dynamics play a substantial role in the temporal and spatial evolution of voids, stiffness, and surface shear strength in

cyclically exposed and submerged soil. Watabe and Sassa (2008) applied multi-channel analysis of surface waves (MASW), proposed by Park et al. (1999) and Hayashi and Suzuki (2004), to identify and describe the stratigraphy of various types of intertidal flats. The tidal flat stratigraphy obtained by means of MASW are consistent with the morphological soil structures, which are considered to be the consequence of the cyclic elastoplastic contraction of the soils that experience a variety of suction dynamics under the tide-induced groundwater table fluctuations. Furthermore, the state of suction in association with the groundwater level is found to be closely linked with the performance of benthic activity (Sassa and Watabe, 2008).

Recently, digital imaging technology has been rapidly developing, and this technology is readily being used in aerial photography for evaluating the coastal environments. Some related studies have been conducted, e.g., aerial survey on geomorphology in a shallow sea by means of aerial digital photography from a helicopter (Tanaka et al.,

2006); aerial survey to identify the distribution of marine forests by means of aerial digital photography from a plane (Ninomiya et al., 2006); and aerial survey by means of digital photography from an unmanned skyhook balloon (Ichimura and Matsubara, 2005).

The aerial survey technology has been developed to create orthophotographs and draw contours. Further, morphological information in coastal areas are captured by an onboard synthetic aperture radar (SAR) installed on an artificial satellite/airplane (Mason et al., 1999). However, it is still difficult to precisely capture morphological information related to intertidal flats because of their extreme flatness. In most cases, the level measurement during the period of exposure or multibeam bathymetry during the period of submergence is alternatively used to obtain the morphological information. In our previous research (Watabe and Sassa, 2008), sediment structures captured by MASW were associated with the morphological structures obtained by level measurement. However, neither bathymetry nor level measurement can capture small fluctuations in the geomorphology of intertidal flats.

In the temporospatial evaluation of morphological fluctuations in intertidal flats, the technical problems with the previous technologies are summarized as follows:

- 1) The accuracy in the level measurement is very high; however, it is very difficult to achieve a sufficient number of measurement points to evaluate the temporospatial variation in geomorphology of the intertidal flats. The soil surface of the intertidal flat should be accessible on foot.
- 2) The bathymetry is applicable to soft muddy flats on which we cannot walk; an onboard equipment on a small craft is used during the period of submergence. The measurement accuracy is not so high. Therefore, we cannot realize sufficient accuracy in order to temporospatially evaluate the geomorphology of the intertidal flats.
- 3) The accuracy of the normal aerial survey is not sufficient to evaluate the geomorphology of the intertidal flats. Because permission is required for a flight, the date/time and number of flights are significantly limited.
- 4) An onboard SAR on an artificial satellite/airplane is available during day and night; however, the shooting date and time are significantly limited and uncontrollable. The accuracy of the survey is not sufficient to evaluate the geomorphology of the intertidal flats.

Temporospatial evaluation of the geomorphology of artificial intertidal flats is very important for the construction, management, and maintenance of ground surface level, because the geomorphology significantly changes in association with not only consolidation but also sediment transportation, immediately after the reclamation work. In addition, because the suction state in association with the groundwater level fluctuations is found to be closely linked with the performance of benthic activity, the importance of temporospatial evaluation of the geomorphology is increasing. Therefore, this study is aimed at developing a new technology for readily and efficiently capturing the temporospatial fluctuations in the geomorphology of intertidal flats. A small intertidal flat with a length of approximately 200 m along the cross-shore direction in an estuary is considered in this study.

On the basis of the above considerations, we attempt to develop a new technology for the geomorphology of intertidal flats by using a small unmanned aerial vehicle (UAV) with equipped a small onboard digital camera. These two equipments have been significantly developed in recent years. Flying small UAVs do not require any permission in Japan; hence, we can obtain aerial photographs at an arbitrary date and time. In addition, we can easily obtain high-resolution aerial photographs from a small UAV in a low altitude flight.

## 2. OVERVIEW OF THE SURVEY

We carried out an aerial survey at the Ena Bay tidal flat in Miura city, Kanagawa Prefecture, Japan on November 1, 2006, by using a small UAV. The dimensions of the tidal flat were suitable for obtaining aerial photographs of the entire area of the flat. According to the astronomical tidal fluctuations, the low tide level was CDL +0.51 m at 7:01, and the high tide level was CDL +1.37 m at 14:01.

The dimensions of the small UAV used in this study were as follows: total length = 1.2 m, total width = 1.7 m, and weight = approximately 2 kg. The UAV was propelled by a motor without noise and exhaust gas. GPS devices, sensors to monitor the flight attitude (accelerometer and gyroscope), a pressure meter, an electronic circuit for flight control, and a small digital camera were installed on to the UAV. The UAV used in this study can be used for autonomous flights around several target points (Suzuki et al., 2007; Tatsumi et al., 2005).

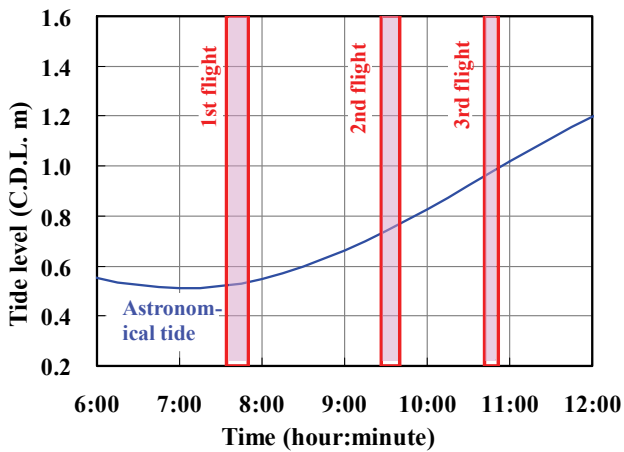


Fig.1. Flight schedule and astronomical tidal fluctuation on November 1, 2006.



Fig.2. Takeoff of the small UAV

We attempted to conduct flights thrice when the water levels were at CDL +0.55 m (7:34 to 7:50), CDL +0.75 m (9:27 to 9:40), and CDL +0.95 m (10:42 to 10:52) during the flooding tide. The duration of each flight was 10–16 min. The relationship between the water level and the flight time is shown in Fig.1.

During the flights, color digital photographs were taken and stored within an interval of 2 or 4 s by the small digital camera. The digital camera used in this study was a marketed product having a capacity to shoot pictures at approximately 6 megapixels (MP).

Figure 2 shows the takeoff of the UAV (at point A in Fig.3). The UAV does not require a runway for takeoff. First, the drive unit is turned on; then, the UAV is launched upwind into the sky; and finally, the autonomous flights are started. The flight route can be modified by using the digital data transmitted from the base station, and the target points and/or flight altitude can be changed. The flight altitude is set at 80 m; however, it is changed to 120 m in the last half of the first flight.

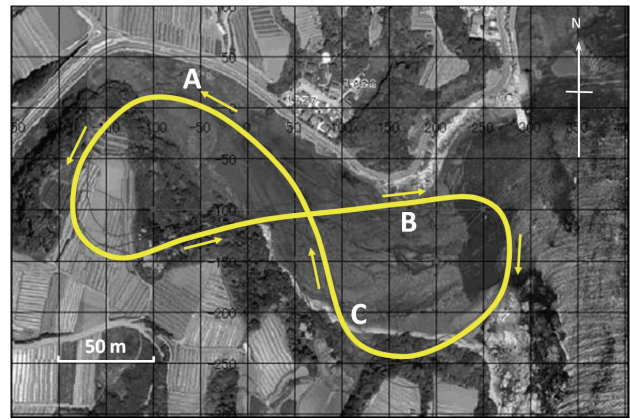


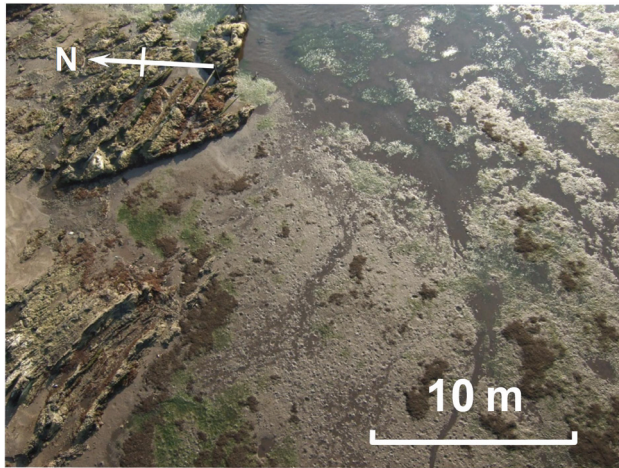
Fig.3. Representative flight route for the UAV aerial survey.

The attitude and position data of the UAV are transmitted to the base station in real time, and these data are recorded on a PC during the flights. Low-resolution aerial photographs monitored by the digital camera are transmitted in real time, and we check whether the photographed area covers the planning area. The high-resolution photographs are saved in the onboard memory of the camera. The target points for the autonomous flight are revised if modification of the flight route is required. In fact, the flight route is slightly modified during the third flight in order to clearly capture the water edge.

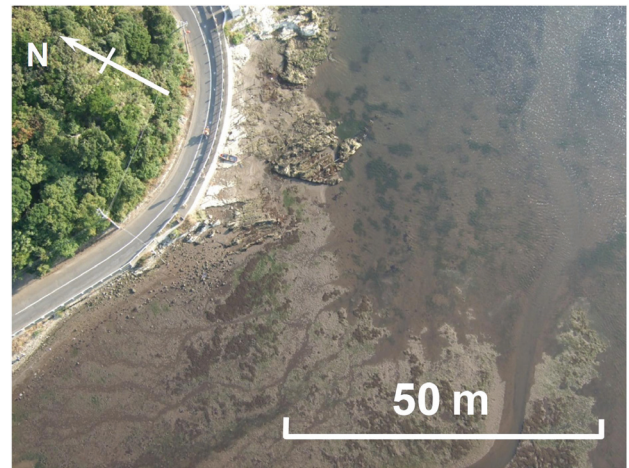
A representative flight route is shown in Fig.3. It was a clear sunny day; however, the sunlight reflection on the water surface is not captured in the aerial photographs, because the position of the sun is low during the morning of the late autumn day. The cruising speed of 60 km/h could overcome the strong east wind of approximately 10 m/s (36 km/h). The point A in Fig.3, i.e., the takeoff and landing point of the UAV, is suitable against the effects of wind as the area is surrounded on three sides by hills.

### 3. RESULTS

Four pictures selected from all the UAV aerial photographs obtained in the first flight are shown in Fig.4: (a) a northern region of the flat photographed at an altitude of 25 m during nose-up flight (near point B in Fig.3); (b) a region including that in photo (a) taken at an altitude of 80 m; (c) a southern region of the flat photographed at an altitude of 80 m (near point C in Fig.3); and (d) a region including that in photo (c) taken at an altitude of 120 m. The UAV aerial photograph taken at an altitude of 25 m has extremely high resolution (one pixel corresponds to approximately a 15-mm square). The UAV aerial photographs taken at an altitude of 80 m are wide the view, but they continue to maintain their high resolutions (one pixel corresponds to approximately



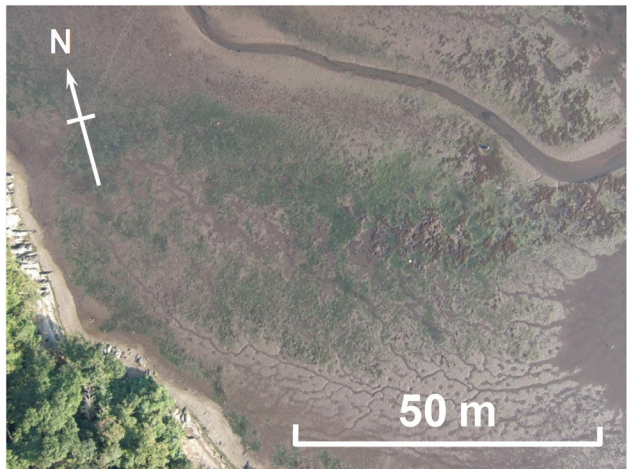
(a) Northern region of the flat: UAV aerial photograph taken at an altitude of 25 m during nose-up flight.



(b) Northern region including (a): UAV aerial photograph taken at an altitude of 80 m.



(c) Southern region of the flat: UAV aerial photograph taken at an altitude of 80 m.



(d) Southern region including (c): UAV aerial photograph taken at an altitude of 120 m.

Fig.4. Examples of UAV aerial photographs taken during the first flight (7:34–7:50).

a 50-mm square). The photograph taken at an altitude of 120 m maintains high resolution (one pixel corresponds to approximately a 70-mm square). In photos (c) and (d), the distribution of sea grasses and geomorphology, including small water routes, are clearly captured.

In the following section, we attempt to integrate the UAV aerial photographs. The UAV aerial photographs were shot at altitudes of 80 and 120 m in the first flight; however, we used the latter because the photographs taken at 120 m covered almost the entire area of the flat. The photographed area for the pictures taken at 120 m altitude is larger than that taken at 80 m; however, the resolutions of the two pictures are almost the same. Integration of the mosaic images can be achieved by either rotation or warping corrections based on the attitude and position data of the UAV.

An integrated image that consists of six photographs taken at an altitude of 120 m during the first flight is shown in Fig.5. This is a simple

integrated image and not an orthophotograph.

The water surface in the intertidal flat, particularly near the water edge, is generally characterized as being tranquil without the influence of ocean waves. In the small-scale intertidal flat considered in this study, the time-lag of tidal fluctuations between the offshore and intertidal zone is negligible. The level of waterline (water edge line) coincides with the tidal water level during the flooding tide in which groundwater does not ooze from the tidal flat surface. This fact implies that the waterline identified in the UAV aerial photograph corresponds to the contour line of the soil surface in the intertidal flat. During the survey, we confirmed this fact as a field situation of the intertidal flat: the waterline gradually moved from the offshore to the onshore during the flooding tide along with the tranquil water surface, although the waves in the open sea were high. The waterline identified at 7:41 corresponds to CDL +55 m.

The waterlines identified at both 9:33 (during the second flight) and 10:44 (during the third flight) are

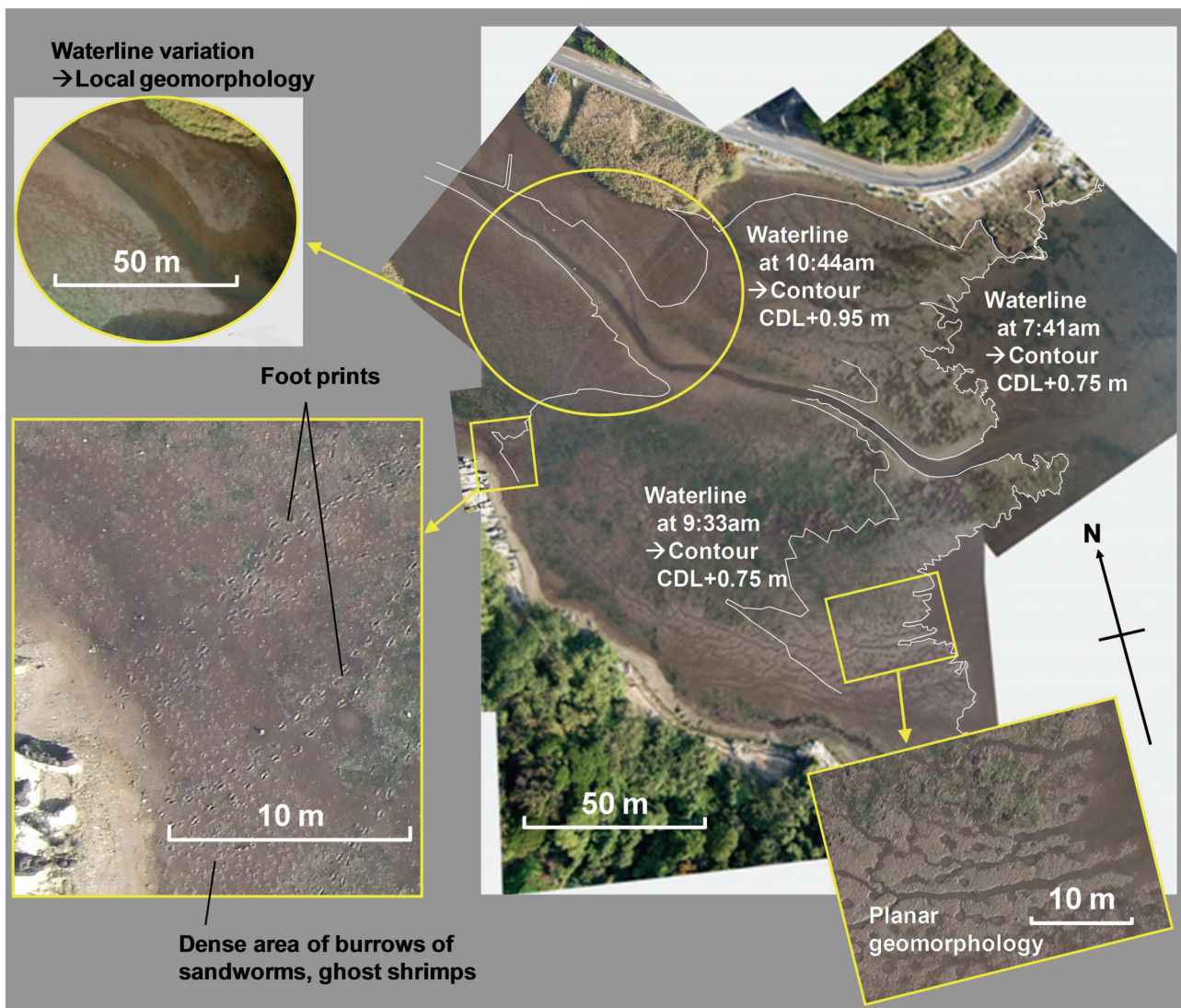


Fig.5. Integrated image of six UAV aerial photographs taken at 7:41 from an altitude of 120 m during the first flight. Waterlines at 7:41 (CDL +0.55 m), 9:33 (CDL +0.75 m), and 10:44 (CDL +0.95 m) are drawn on the image. The enlarged image on the lower-right-hand side shows small water routes connecting benthic burrows. The enlarged image on the lower-left-hand side shows the distribution of benthic burrows shown on the soil surface. The upper-left-hand side image shows the seine of the upstream of the water channel at 10:44.

also shown in Fig.5. These two waterlines correspond to approximately CDL +0.75 m and CDL +0.95 m. We can see that the interval between the two contours identified at 7:41 and 9:33 (approximately 30 m) is narrower than that between the contours identified at 9:33 and 10:44 (approximately 70 m). Although the tidal flat is apparently very flat, the surface has a mild slope, which becomes steeper along the offshore direction. In addition, the width of the water channel at the upper stream region photographed at 10:44 is significantly widened; however, the waterline varies only on the northern region. This fact indicates that the UAV aerial photographs are useful for understanding the local geomorphology, which describes that the slope on the north side is mild but the slope on the south side is steep.

As mentioned above, we can precisely and

efficiently capture the geomorphology of very flat intertidal flats by identifying the waterline variation from UAV aerial photographs, because the water surface near the water edge in the intertidal flats is significantly tranquil. The technology is also useful for investigating the temporospatial variation in the geomorphology of intertidal flats, because the UAV can repeatedly fly along the same route by using the autonomous navigation system. UAV aerial photography is applicable to not only natural flats but also artificial flats for the management of ground surface level.

The high-resolution UAV aerial photographs precisely capture geomorphology, areas covered by sea grasses, burrows created by benthic activities, small water routes connecting the burrows, etc. The small water routes connecting the burrows probably create a large water channel. It may be possible to

capture the process of morphological formation, when a series of UAV aerial surveys are carried out periodically, e.g., weekly, monthly, seasonally, and yearly.

We can observe some green areas covered by sea grasses on the southern half region from the water channel (lower half of the photograph). From the enlarged photograph, which was taken at an altitude of 80 m, shown on the lower-left-hand side of Fig.5, we can identify some areas covered by abundant burrows of sandworms and ghost shrimps in high density on exposed and wet regions rather than dry or submerged regions. In comparison with the foot prints up to a distance of approximately 27 cm, we can identify subjects within a dimension of a few centimeter squares, such as small burrows of benthic activities. The resolution of the UAV aerial photographs can be improved by a flight at a lower altitude. In addition, the rapid development of digital technology may contribute toward significant improvement in the specifications of commercial compact digital cameras, which means that the resolution of the aerial photographs obtained using the UAV technology will be continuously improved in the future. Because we have found out that the benthic activities are closely linked to the geoenvironmental dynamics (Sassa and Watabe, 2008), it is very interesting to study the link between the geomorphology and benthic activities in intertidal flats by using high-resolution UAV aerial photographs from which we can study the distributions of both water retention conditions and burrowing densities.

In this study, we used a small UAV that resembles a plane; however, alternative options are available, such as a UAV resembling a helicopter (e.g., Nagai et al., 2005). Further, the methods to precisely and efficiently integrate several mosaic images are being developed (Haraguchi et al., 2006). Therefore, we can expect that UAV aerial digital photography will be an ordinary and useful technology in the near future.

#### 4. SUMMARY

We attempted to use UAV aerial photography for studying a small intertidal flat. We integrated some photographs, and then we precisely and efficiently captured the geomorphology of the intertidal flat by identifying the waterline variation, because the water surface near the water edge in the intertidal flat was significantly tranquil. This technology is applicable to not only natural flats but also artificial flats for the management of ground surface level.

High-resolution UAV aerial photographs in which benthic burrows can be identified are expected to be extensively used in studies aimed at finding the link between the geomorphology and benthic activities in intertidal flats.

**ACKNOWLEDGMENT:** This study was supported by the Grant-in-Aid for Scientific Research (No. 18360232) from the Ministry of Education, Culture, Sports, Science and Technology, Japan. Further, the field survey conducted by using the small UAV was carried out in collaboration with the Mitsubishi Electric Co., Ltd.

#### REFERENCES

- 1) Haraguchi, K., Meguro, J., Takiguchi, J., Sato, K., Hatayama, M., Amano, Y. and Hashizume, T.: High resolution mosaic images obtained by small autonomous aerial vehicle and temporospatial GIS, Proceedings of Annual Conference on System Integration Division, Japan Society of Instrument and Control Engineers, pp.896-897, 2006. (in Japanese)
- 2) Hayashi, K., Suzuki, H., 2004. CMP cross-correlation analysis of multi-channel surface-wave data. *Exploration Geophysics*. 35, 7–13.
- 3) Ichimura, Y. and Matsubara, Y.: A study on the development of the mapping system of the coast, *Annual Journal of Coastal Engineering*, Japan Society of Civil Engineers, Vol.52, pp.1436-1440, 2005. (in Japanese)
- 4) Mason, D.C., Amin, M., Davenport, I.J., Flather, R.A., Robinson, G.J. and Smith, J.A.: Measurement of recent intertidal sediment transport in Morecambe Bay using the waterline method, *Estuarine, Coastal and Shelf Science*, Vol.49, pp.427-456, 1999.
- 5) Nagai, M., Shibusaki, R., Chen, T., Kumagai, H. and Mizukami, S.: UAV borne 3D Mapping System based on Multi-Sensor Integration, *Journal of the Japan Society of Photogrammetry and Remote Sensing*, Vol.44, No.6, pp.58-67, 2005. (in Japanese)
- 6) Ninomiya, J., N. Mori, N. and Yamochi, S.: Remote sensing of sea grass coverage using optical transfer theory, *Annual Journal of Coastal Engineering*, Japan Society of Civil Engineers, Vol.53, pp.1426-1430, 2006. (in Japanese)
- 7) Park, C.B., Miller, R.D., Xia, J.: Multichannel analysis of surface waves. *Geophysics*, 64(3), 800–808, 1999.
- 8) Sassa, S. and Watabe, Y.: Role of suction dynamics in evolution of intertidal sandy flats: Field evidence, experiments, and theoretical model, *Journal of Geophysical Research*, 112, F01003, 2007. doi:10.1029/2006JF000575
- 9) Sassa, S. and Watabe, Y.: Threshold, optimum and critical geoenvironmental conditions for burrowing activity of sand bubbler crab *Scopimera globosa*, *Marine Ecology Progress Series*, Vol.354, pp.191-199, 2008. doi:10.3354/meps07236.
- 10) Suzuki, T., Meguro, J., Amano, Y., Hashizume, T., Takiguchi, J., Sato, K. and Hatayama, M.: High accuracy 3D measurement by a small unmanned aerial vehicle, *Proceedings of Robotics and Mechatronics Conference 2007*, Japan Society of Mechanical Engineers, 2A2-B05, 2007. (in Japanese)
- 11) Tanaka, R., Nishi, R., Yuki, T. and Futatsumachi, S.: Photographic survey in a sub-aquatic region applying commercially available digital camera, *Annual Journal of Civil Engineering in the Ocean*, Japan Society of Civil Engineers, Vol.22, pp.911-915, 2006. (in Japanese)
- 12) Tatsumi, K., Hirokawa, R., Hiromatsu, Y., Suzuki, S.,

Tsuchiya, T. and Kubo, D.: Development of small autonomous flying robot system and its test flight, Journal of the Japan Society for Aeronautical and Space Sciences, Vol.54-625, pp.41-45, 2005. (in Japanese)

13) Watabe, Y. and Sassa, S.: Application of MASW technology to identification of tidal flat stratigraphy and its geoenvironmental interpretation, Marine Geology, Vol.252, pp.79-88, 2008. doi: 10.1016/j.margeo.2008.03.007